TOPICAL REVIEW — 2D materials: physics and device applications

Two-dimensional materials for ultrafast lasers*

Fengqiu Wang(王枫秋)†

School of Electronic Science and Engineering and Collaborative Innovation Center of Advanced Microstructures, Nanjing University, Nanjing 210093, *China*

(Received 17 October 2016; revised manuscript received 4 November 2016; published online 13 February 2017)

As the fundamental optical properties and novel photophysics of graphene and related two-dimensional (2D) crystals are being extensively investigated and revealed, a range of potential applications in optical and optoelectronic devices have been proposed and demonstrated. Of the many possibilities, the use of 2D materials as broadband, cost-effective and versatile ultrafast optical switches (or saturable absorbers) for short-pulsed lasers constitutes a rapidly developing field with not only a good number of publications, but also a promising prospect for commercial exploitation. This review primarily focuses on the recent development of pulsed lasers based on several representative 2D materials. The comparative advantages of these materials are discussed, and challenges to practical exploitation, which represent good future directions of research, are laid out.

Keywords: ultrafast lasers, mode-locking, *Q*-switching, graphene, transition metal dichalcogenides, black phosphorus, topological insulators

PACS: 42.65.–k, 78.47.J–, 42.65.Re, 78.67.Wj **DOI:** 10.1088/1674-1056/26/3/034202

1. Introduction

Ultrafast science is a highly interdisciplinary research area that encompasses laser physics, materials science, nanotechnology and biomedical research.[1–5] Today, ultrafast lasers can routinely generate pulses on the femtosecond scale, and advanced systems employing nonlinear optical techniques can produce durations down to several tens of an attosecond.[6,7] These ultrafast systems are playing increasingly important roles across a broad range of science and engineering subjects, enabling not only ever more profound knowledge about ultrafast physical, chemical and biological phenomena, but also orders of magnitude improvement in our manufacturing and metrological capabilities.[8–10] While the theoretical foundation of ultrafast pulse generation in mode-locked lasers was laid several decades ago,[11] the quest for ultrafast lasers with continuously improved performance, i.e., shorter pulse duration, wider spectral access, higher output power, and better noise characteristics, has never stopped.[12–14]

Of the many available techniques for ultrashort-pulse generation, passive mode-locking represents the state-of-the-art for enabling extremely short pulses.[3] The key operation principle of passive mode-locking involves the use of a nonlinear optical material or device, known as a saturable absorber (SA), which can transit between different absorption states on an ultrafast timescale, upon excitation by a high intensity light field.[15] The passive saturable absorber induces a periodic modulation of the circulating light field in the laser cavity, causing a large number of longitudinal modes to oscillate in phase, thereby forming a regular train of short pulses in the time domain.[11] The underlying mechanism for saturable absorption can be remarkably simple, typically based on Pauli exclusion principles,[16] i.e., the absorption of a material would decrease if a proportionally large number of electrons are found in the upper excited states, although other physical mechanisms can also lead to a similar overall effect.

Throughout the past few decades, a number of materials have been identified and developed as saturable absorbers, including organic dyes, colour centers, as well as transition metal and rare earth ions.[17–19] However, these early materials are not ideal. For example, organic dyes are usually difficult to handle in a laser cavity and are susceptible to optical damage. Ion-based saturable absorbers are typically employed in the form of doped glass/crystal films with relatively high losses due to unavoidable bulk optical coupling, which prevents wide use in solid-state and semiconductor lasers. An artificial saturable absorber effect known as the Kerr lens was discovered in 1991 by Sibbett and co-workers,[20] and subsequently led to the successful commercialization of the solid-state Ti: sapphire lasers. However, the Kerr lens is an extremely fast SA with a response time around a few femtoseconds. Such a transient characteristics is difficult to tune as it arises from the intrinsic dielectric response of the crystal. This was known to cause difficulty for the mode-locked laser to self-start, presenting an undesirable feature for practical systems.[3] The advent of the semiconductor saturable absorber mirror (SESAM), invented in the early 1990s by Bell

*Project supported by the National Natural Science Foundation of China (Grant Nos. 61378025 and 61427812), the Shuangchuang Team Program of Jiangsu Province, China, the National Key Basic Research Program of China (Grant No. 2014CB921101), and the State Key Laboratory of Advanced Optical Communication Systems Networks, China.

†Corresponding author. E-mail: fwang@nju.edu.cn

Labs researchers, successfully worked around such a technical problem and since its introduction, SESAMs have been routinely used to initiate mode-locking in Kerr lens mode-locked Ti:sapphire lasers.[21] Before long, with advances in multiple quantum-well design and growth techniques, many key optical parameters of SESAMs were found capable of being flexibly customized. In particular, through low-temperature growth or post-growth processing, the carrier relaxation times, which not only critically govern the initial pulse formation processes, but also directly affect the saturation fluence of the saturable absorbers, could be broadly tailored within a range from a few picoseconds to nanoseconds.[22,23] The saturation fluence or intensity of the device can also be tuned by customizing the top reflective mirror or by precise engineering of the composition of the absorber layer.[15] Thanks to these technical advances, SESAM has established itself as the most prevalent absorber technology for solid-state, fiber and semiconductor lasers, enabling significant optimization of near-infrared lasers and making them the work horses for today's ultrafast science exploration.[3] Despite the technical prowess, SESAMs have a known drawback. Due to the use of conventional semiconductor materials and optical resonant structures, the operation range of SESAMs is limited to the near-infrared range, typically below 2 μm (while the nonlinear optical bandwidth is $\sim$ 100 nm about the design wavelength). Scaling the operation wavelength of SESAMs further into the mid-infrared, i.e. beyond 3 μm, remains elusive. The quest for an alternative saturable absorber technology that can address these limitations while retaining the key benefits of SESAMs remains an important research topic for the ultrafast laser community.

Single- and few-layer 2D crystals have received significant attention since the isolation of graphene in 2004.[24] Due to the unique low-dimensional physics, a range of emerging 2D materials have been used in the development of next-generation photonics and optoelectronic technologies. Of the many possibilities, the use of 2D materials as broadband, cost-effective and versatile ultrafast optical switches (or saturable absorbers) for short-pulsed lasers constitutes a rapidly developing field with not only a good number of publications, but also a promising prospect for commercial exploitation. In the following, we briefly review recent results of short-pulsed lasers enabled by a few representative two-dimensional materials, covering graphene, transition metal dichalcogenides, and black phosphorus in turn. It should be noted that due to the large number of reports in the literature, this review is not intended to be exhaustive, but rather efforts are made to highlight the most significant recent results, to discuss the comparative advantages of different materials (especially those of broad relevance to optical and optoelectronic applications), and to point out remaining technical challenges to overcome for practical exploitation.

2. Two-dimensional-material-enabled short-pulsed lasers

2.1. Graphene

Graphene is a flat monolayer of carbon atoms tightly arranged into a two-dimensional honeycomb lattice, and is a basic building block for graphite. Since its successful isolation in 2004, graphene has quickly emerged as the most promising material for nanoelectronics and nanophotonics. The electronic and optical properties of graphene as well as the roadmap for its technological development are summarized in a few recent review papers.[25–28] Graphene was first employed for the mode-locking of lasers independently by two groups.[29–31] Compared with carbon nanotubes, which have similar atomic arrangement and have been identified earlier as a broadband saturable absorber material,[31–33] graphene exhibits additional advantages in terms of operating bandwidth, uniform nonlinear optical response over broad spectral region, as well as ease of integration into photonic components and systems. While carbon nanotubes are most often used in the form of polymer composites, the fact that large-scale, high-quality crystalline graphene can be grown on copper foil using chemical vapor deposition (CVD) method and can subsequently be flexibly transferred to arbitrary optical substrates makes graphene highly adaptable for various laser formats. Thus far, graphene has been used to mode-lock fiber,[29–31,34–39] solid-state,[40–44] waveguide,[45] and semiconductor lasers.[46,47] A few comprehensive reviews of graphene-based saturable absorber devices are available.[48–50] Graphene derivatives, including graphene oxide and reduced graphene oxide, also exhibit ultrafast optical properties and can enable pulsed laser mode-locking. However, the necessity of additional chemical/physical processing renders the fabrication less well controlled and in the meantime unavoidably introduces a considerable amount of defects and gap-states.[51] Among various 2D materials, graphene has thus far demonstrated performance levels most comparable to or even better than conventional semiconductor devices and it has also shown the best adaptability for fulfilling requirements of a wide range of laser formats.

Similar to broadband operations of SWNTs,[52–54] graphene absorbers have been shown to enable broadly tunable Q-switched and mode-locked operations.[34,35] Yang and co-workers used a CVD-grown multilayer graphene SA ($>$ 5 layer) to mode-lock three different lasers, including ytterbium-, erbium-, and thulium-doped fiber cavities, convincingly validating the intrinsic broadband feature of graphene flakes.[36] Sotor *et al.* demonstrated a passively synchronized thulium- and erbium-doped fiber laser by a common graphene SA, where soliton operations were simultaneously achieved at 1559 and 1938 nm, respectively.[37] Such synchronous lasers could be extremely useful for different-

frequency generation (DFG) for mid-infrared operation beyond 3 μm. In terms of repetition rate scaling, the highest repetition was achieved based on a short-cavity fiber laser by Martinez and co-workers, where a repetition rate of 20 GHz is achieved through careful optimization of the gain and loss of a miniaturized FP cavity.[38] Zhang and co-workers demonstrated for the first time mode-locked operation other than conventional soliton regime, i.e., dissipative soliton operation, validating the versatility of graphene SA for various pulsation regimes.[39]

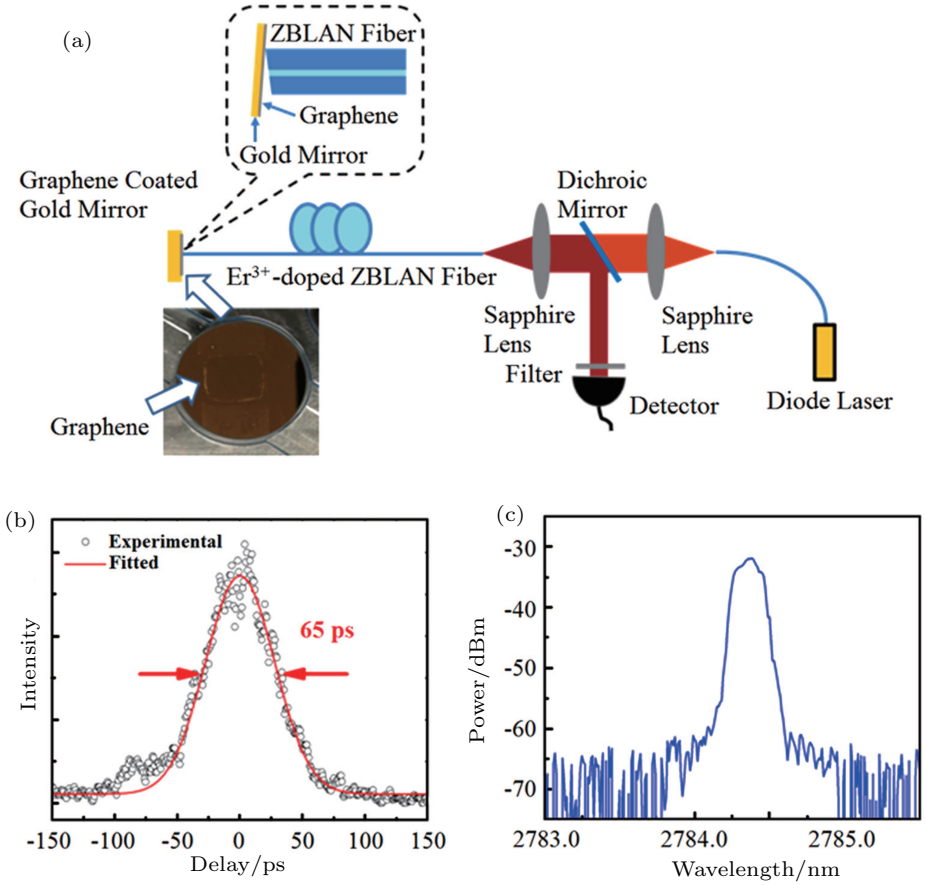

Fig. 1. (color online) Graphene mode-locked mid-infrared pulsed fiber laser. (a) Er^{3+}-doped ZBLAN fiber laser incorporating a multi-layer graphene mirror as a saturable absorber. (b) Measured autocorrelation trace showing a FWHM (full-width-half-maximum) pulse width of ~ 65 ps. Assuming a sech^2 profile, this yields a pulse duration of ~ 42 ps. (c) Optical spectrum of the mode-locked laser, showing a mid-IR center wavelength of $\sim$2.78 μm.[58]

While early studies are mainly focused on the conventional near-infrared band, recent efforts have shifted towards the use of graphene for long-wavelength lasers, especially those around 2 μm and beyond.[55–63] The exploration of graphene-based mid-infrared fiber lasers started in 2012, with several groups reporting pulsed laser operations around 2 μm. For fiber lasers, liquid phase exfoliated (LPE) graphene-based composite films were first used to demonstrate a *Q*-switched laser[55] and a mode-locked thulium fiber laser,[56] respectively. Wei and co-workers demonstrated the first graphene-based pulsed laser operation at a wavelength close to 3 μm, where graphene was deposited onto a fiber ferrule mirror using the optically-driven deposition method.[57] The laser emitted 2.9 μs pulses with a pulse energy up to 1.67 μJ. By optimizing the fiber laser cavity and using a multi-layer graphene-covered gold mirror, mode-locked operation at a wavelength of 2.8 μm with a pulse duration $\sim$ 42 ps was demonstrated (see Fig. 1).[58] This is the longest laser wavelength at which graphene-based passive mode-locking has been demonstrated to date. The first use of CVD-grown graphene for mode-locking solid-state lasers in the mid-infrared was demonstrated by Xie and co-workers, where a Tm: CLNGG gain media was used to generate 60 mW, 729 fs pulses at a wavelength of 2018 nm.[43] Graphene was transferred onto a dielectric mirror and the device was operated in the reflectance mode as a cavity end mirror.[43] By transferring graphene to a transparent dielectric substrate, a Tm:Lu_2O_3 crystal laser was mode-locked in such a way that shorter ($\sim$ 410 fs) and more powerful ($\sim$ 270 mW) pulses were obtained.[44] Thus far, the longest wavelength, graphene-enabled, mode-locked, solid-state laser is based on a Cr:ZnSe laser, operating at 2500 nm, in which graphene transferred onto a CaF_2 substrate acted as an absorber in the transmission mode.[59] The laser features a further reduced pulse duration of 226 fs, with 80 mW

output power. Via careful intra-cavity dispersion compensation, Sorokina and co-workers achieved the shortest mid-infrared pulse duration for graphene-based pulsed lasers. The 41 fs duration corresponds to only 5.1 optical cycles.[60] Recently, Cho and co-workers employed a CVD grown monolayer graphene SA to mode-lock a solid-state Cr^{2+}:ZnS laser. The laser exhibits a broad tuning range from 2120 nm to 2408 nm (see Fig. 2). This represents the widest tuning range for graphene-based, mode-locked laser (300 nm, > 10% of the center wavelength).[62] In addition, the relaxation dynamics of monolayer graphene is measured at 2.35 μm where a fast recover time ∼ 240 fs and a slower component ∼ 2.4 ps were obtained.[62] Graphene-based SA devices can take other forms such as those directly deposited on SiC substrates. *Q*-switched operation of a Tm:YAG laser was demonstrated using such an approach.[63]

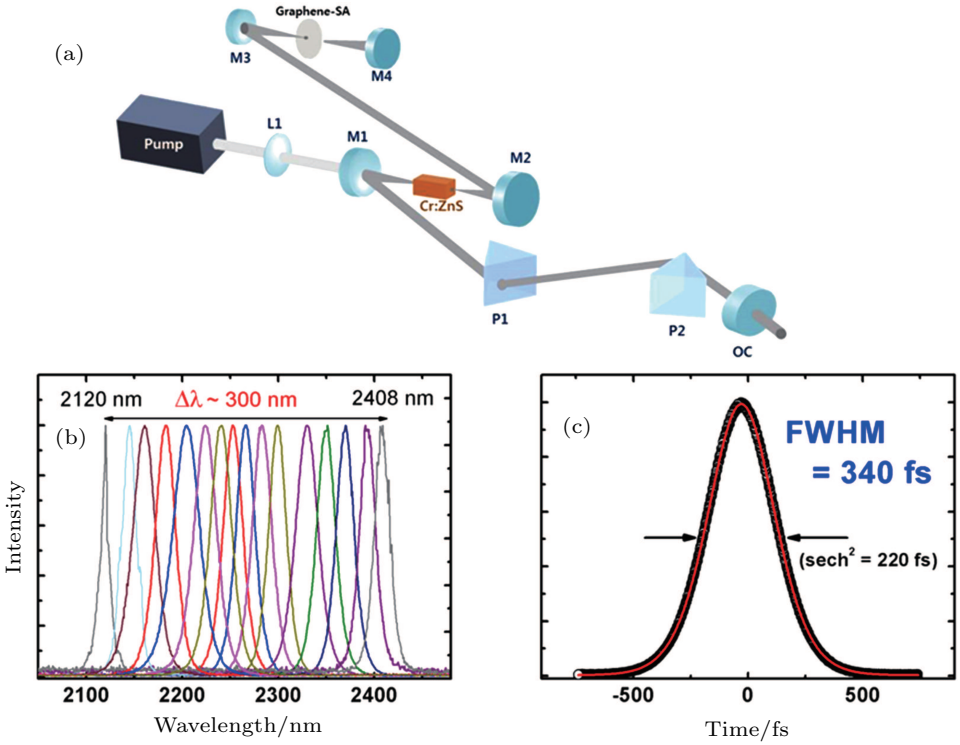

Fig. 2. (color online) (a) Schematic of the graphene mode-locked broadly tunable Cr:ZnSe laser. (b) The optical spectra showing an ultra-broad tuning range of ∼ 300 nm, from 2120 nm to 2408 nm. (c) The autocorrelation trace showing a pulse duration ∼ 340 fs.[62]

Flexibility in controlling the optical parameters, such as linear absorption, relaxation times, modulation depth, etc., is an important aspect for engineering practical SA devices and the availability of a large parameter space would allow for adequate optimization of SA-enabled, pulsed laser regimes. Indeed, SESAM has been the most capable of SA devices in terms of parameter customizations. The gate-tunable feature of graphene makes it an excellent choice for an electrically-tunable SA, which may provide multiple benefits for laser operations, including actively controlling the operating regime of a pulsed laser.[64] Rotermund, Yeom, and co-workers demonstrated an electrically manipulable in-line graphene SA device by integrating graphene-based field effect transistors on a side-polished fiber (SPF) (see Fig. 3(a)).[65] The device exhibits significant (> 90%) optical transmission change and shows continuous tuning of the nonlinear saturable absorber characteristics, i.e., the modulation depth (see Fig. 3(b)). Due to good compatibility with fiber-optic system, the in-line graphene SA was used in an Er fiber ring cavity for a switchable pulsed laser where the control voltage can be employed to switch between the *Q*-switched state (pulse duration, 3.5 μs; repetition rate, 25.4 kHz; gate voltage −0.18 V) and the mode-locked state (pulse duration, 423 fs; repetition rate, 30.9 MHz; gate voltage −1.05 V). Sennaroglu and co-workers reported a graphene supercapacitor device as a voltage-controlled SA.[66] The device was then operated at bias voltages of 0.5 V–1 V to generate sub-100 fs pulses from a Cr^{4+}:forsterite laser operating at 1255 nm (see Figs. 3(c) and 3(d)). It should be pointed out that although modulation depth is sensitively dependent on the control voltage, the relaxation time constants, which may have strong impact on the initialization of mode-locked operations, are not directly amendable by the externally applied voltage. For SESAMs, both low-temperature growth and post-growth implantation have been applied to tune the relaxation time, through the introduction of lattice defects.[67,68]

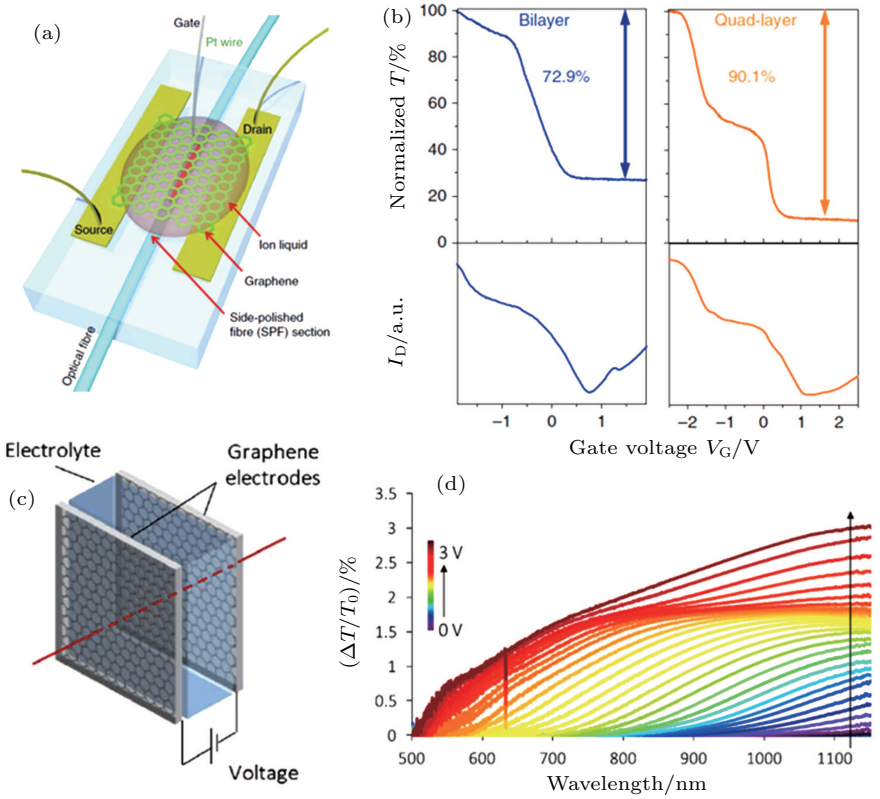

Fig. 3. (color online) (a) Schematic diagram of gate-variable all-fibre graphene device. The side-polished fiber (SPF) was fabricated using a standard single-mode optical fiber where two metal electrodes were deposited with 50-nm thickness at both sides of the side-polished region. After transferring the graphene layer, ion liquid was applied to the graphene. Two electrodes and a Pt wire were used as source, drain and gate, respectively.[65] (b) Gate-controlled optical properties of all-fiber devices with bi-(left panels) and quad-layer (right panels) graphene. The bottom panels correspond to electrical transport properties of devices with bi- and quad-layer graphene.[65] (c) Schematic of the voltage-controlled graphene SA based on the supercapacitor structure.[66] (d) Variation of the normalized change of the optical transmission of the graphene as a function of the wavelength at different bias voltages in the 0–3 V range.[66]

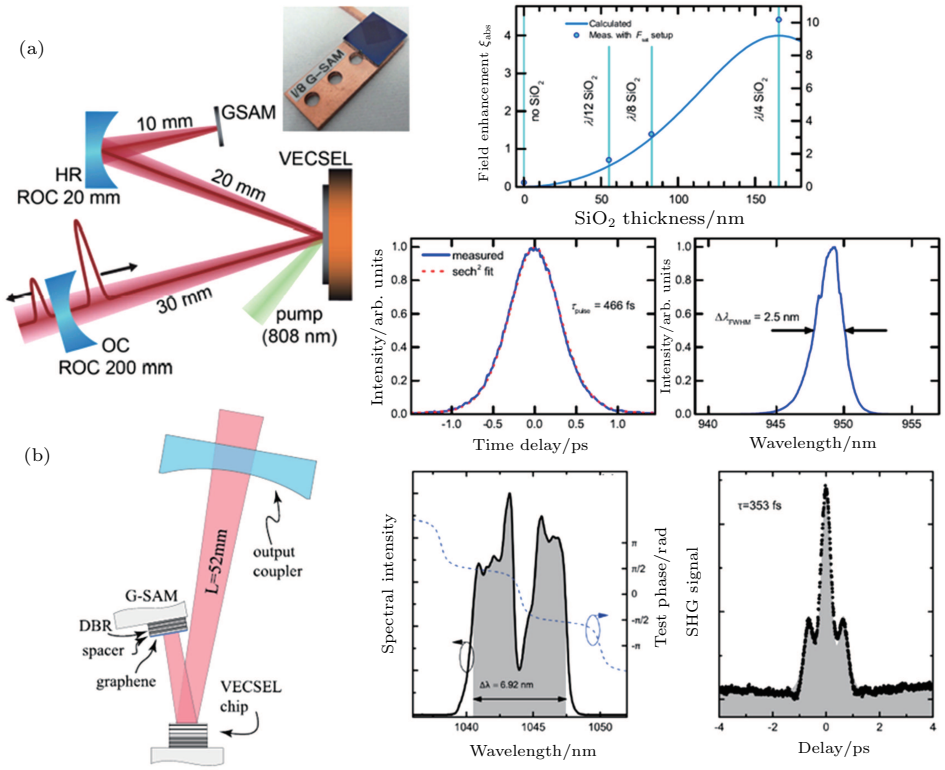

Fig. 4. (color online) (a) Schematic of the graphene SA mode-locked VECSEL setup (left). Linear absorption and field intensity enhancement at the single-layer graphene location corresponding to the DBRs without SiO_2 ($\xi_{abs} = 0$), a $\lambda/12$ layer of SiO2 ($\xi_{abs} = 0.5$), a $\lambda/8$ layer ($\xi_{abs} = 1.3$), and a $\lambda/4$ layer ($\xi_{abs} = 4$) (right-top). Mode-locking results showing the autocorrelation trace, corresponding to a pulse duration of 466 fs, and the optical spectrum (right-bottom).[46] (b) The schematic of the V-cavity with the gain chip at the fold and the graphene SA mirror and outcoupler at either end (left). The optical spectrum of the VECSEL cavity operating at 9.3 W, with a spectral bandwidth of 6.92 nm (middle) and the corresponding autocorrelation trace (right).[47]

Novel approaches to tune the relaxation time of graphene are to be developed and would further expand the versatility of graphene-based optical devices, pertinent not only to saturable absorbers but also to photodetectors, solar cells, as well as light-emitting devices. Apart from the active approaches, passive ways of adjusting the graphene SA's parameters have also been demonstrated through fine tuning the thickness of a spacer between a single-layer graphene and a high-reflection mirror (see Fig. 4). Due to the interference between the incident and reflected light field at the mirror, graphene's field intensity enhancement can be continuously adjusted between 0 and 400%. With such a flexible graphene SA, a VECSEL is successfully mode-locked and wavelength-tunable operation can be achieved across 935 nm to 981 nm.[47]

2.2. Transition metal dichalcogenides (TMDs)

Transition metal dichalcogenides – layered crystals comprising X–M–X sheets (where X = S, Se, Te and M = Mo, W) bound by weak van der Waals forces – have enjoyed a renaissance as a consequence of the explosive growth in nanoelectronics and nanophotonics research.[69–72] Distinct from graphene, TMDs can be semiconducting exhibiting a layer-dependent bandgap, ranging from indirect in bulk form to direct in monolayer crystals.[73] On one hand, the reduced dimensionality and the associated reduced dielectric screening of Coulomb interactions between charge carriers lead to extremely strong excitonic effects in TMDs.[74,75] Theoretical calculations have predicted very large exciton binding energies in the range of 0.5–1 eV for monolayer TMDs.[76] The excitonic nature of photoexcitation in TMDs provides enhanced light absorption which is very useful for saturable absorbers where higher modulation depth is needed, such as in the case of fiber lasers. On the other hand, the breaking of inversion symmetry and strong spin–orbit coupling in TMDs lead to valley-selective circular dichroism, and have resulted in a number of novel device concepts.[69–71] It should be mentioned that TMDs exhibit a rather rich and complex photophysics, i.e., multiple physical mechanisms may operate simultaneously to govern the ultrafast and nonlinear optical response of the material. Recently, several groups experimentally identified the presence of giant and ultrafast bandgap renormalization (BGR) effect in TMDs upon intense ultrashort pulse irradiation. The effect which is induced by the Mott transition from excitonic states to free-carriers in the 2D system opens up an exciting new route for realizing optical controlled functionalities, i.e., ultrafast all-optical modulators (see Fig. 5).[77–79] On the other hand, Kumar and co-workers observed a strong density-dependent decay of the excitons in monolayer $MoSe_2$ in the initial phase (within 50 ps) of the transient relaxation, i.e., higher exciton injection density (or pump fluence) would lead to a faster initial decay component. The effect can be well accounted for by considering an exciton–exciton annihilation rate of 0.33 ± 0.06 cm^2/s, suggesting strong interaction between excitons in this strongly confined system. Such a feature was not observed in a bulk sample under similar conditions.[80] A similar effect was also observed in monolayer MoS_2, where an exciton–exciton annihilation rate of 0.043 ± 0.011 cm^2/s was experimentally derived.[81] These transient dynamics of the excitonic features could have a profound impact on TMD-based optical and optoelectronic devices.[77–81] Quite a few studies of the ultrafast photocarrier dynamics in TMDs have been reported based on optical pump-probe spectroscopy.[82–86] Ultrafast photoresponses of TMDs are found to depend on a number of factors, including microscopic morphologies, substrates, excitation species, as well as the number of layers. The importance of these studies is to reveal fundamental behaviours of photoexcitation species in these emerging 2D systems on one hand, and on the other hand to provide guidelines for realizing robust and reliable tuning of the relaxation times of such materials, which play a significant role in the build-up phase of mode-locked pulses. For mechanically-exfoliated MoS_2 flakes, the relaxation times are found to be relatively long, in the range of $\sim100\pm10$ ps on a SiO_2/Si substrate,[82] and $\sim 850 \pm 48$ ps for a suspended sample.[83] The dynamics shows completely different features for liquid phase exfoliated TMD nanosheets, which exhibit an ultrafast initial photobleaching (PB) signature followed by a transition to photoinduced absorption (PA) signature.[84] By using an ultrashort pump pulse of $\sim$ 10 fs and by using pump fluence above the 2D Mott density of MoS_2, i.e. in the range of 10^{13}–10^{14} cm^{-2}, Nie and co-workers revealed that the carrier thermalization and subsequent cooling dynamics are on $<$ 20 fs and $\sim$ 0.6 ps timescales respectively.[85] Wang and co-workers studied carrier dynamics of few-layer MoS_2 and found that the carrier recovery time increases dramatically from $\sim$ 50 ps in monolayer to $\sim$ 1 ns in 10-layer MoS_2.[86] The results are consistent with defect-assisted carrier recombination and represent a meaningful way of tuning the photocarrier recombination through scaling the layer number in few-layer MoS_2. (see Fig. 6). These extrinsic factors pose a challenge for practical exploitation of TMDs. Compared with pump-probe investigations typically carried out in the non-degenerate configuration, transient response in the degenerate configuration may directly yield insights about their saturable absorber behaviour.[87] Broadband nonlinear absorption measurement performed on a CVD-grown single crystal $MoSe_2$ flake (on a silver mirror) recently yielded uniform nonlinear optical response over the broad wavelength range covering the A-exciton resonance, where a constant modulation depth of $\sim$ 80% and saturation intensity $\sim$ 2.5 MW/cm^2 were inferred (Fig. 7).[88] An immediate benefit of such an unexpected spectral response of TMDs is the possibility of engineering a device with precisely pre-defined nonlinear optical properties over a broad optical range, which has proved difficult for most semiconductor-based devices including SESAMs and SWNTs.

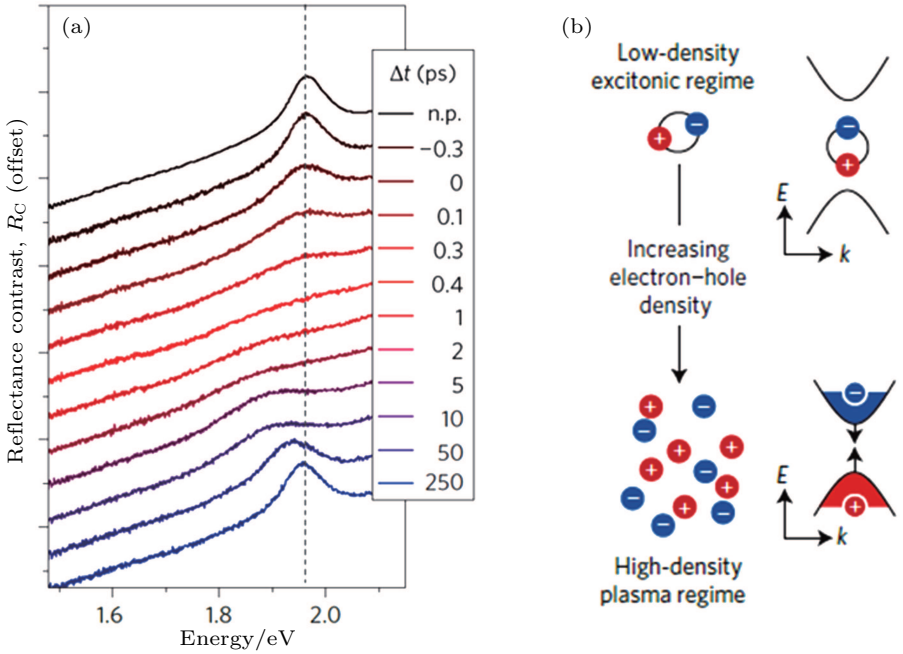

Fig. 5. (color online) (a) Reflectance contrast spectra of a WS_2 layer at different time delays after excitation, vertically offset for clarity (n.p. denotes the spectrum without pump excitation), showing the evolution of the spectra. The initial bleaching of the exciton peak and inversion both develop instantaneously within the experimental resolution of 0.4 ps, indicating that initial relaxation processes occur on the 100 fs timescale. After ~ 250 ps, the optical response fully returns to the initial condition. (b) Illustration of the transition from the low-density excitonic regime to a dense electron–hole plasma.[78]

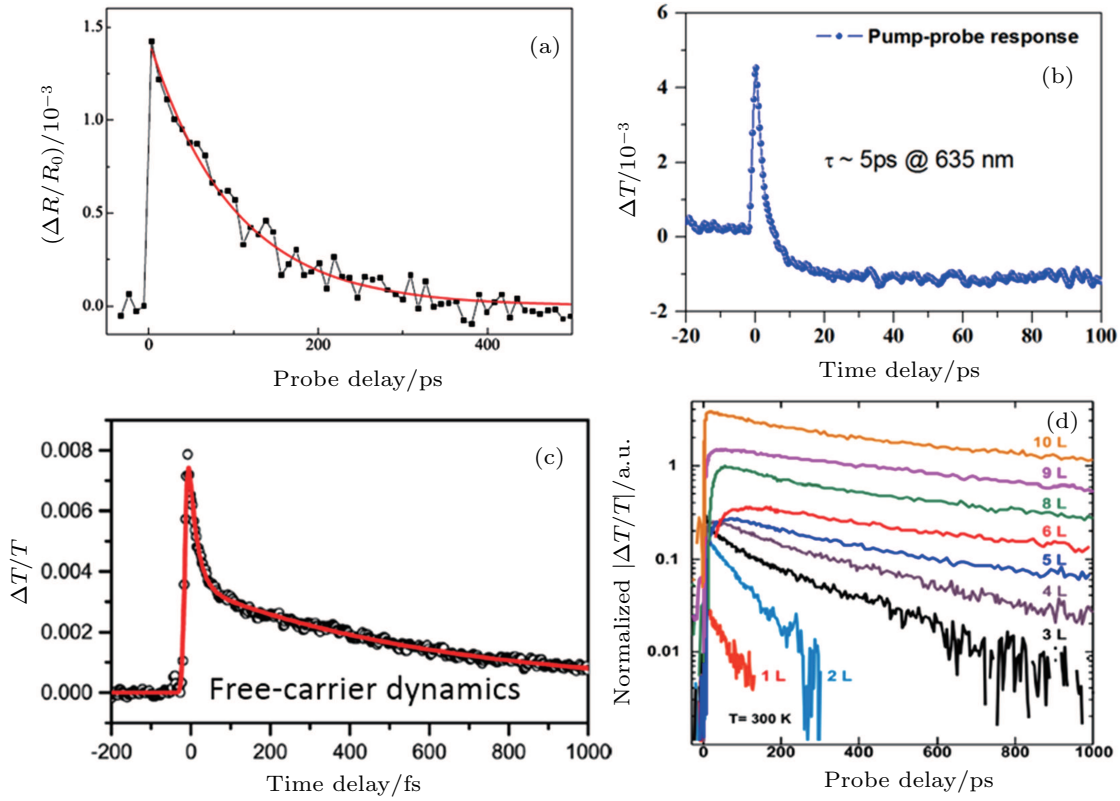

Fig. 6. (color online) (a) Pump-probe spectroscopy performed with 390 nm pump and 660 nm probe on a mechanically exfoliated MoS_2 sample (transferred onto a SO_2/Si substrate), showing a carrier lifetime of 100±10 ps.[83] (b) Time-resolved differential transmission spectra performed on a liquid phase exfoliated few-layer WS_2 sample with degenerate 635 nm pump and probe beam, showing a fast PB signal (~ 5 ps), followed by an emerging PA signature.[84] (c) Transient differential transmission performed with 10 fs visible pulses on a few-layer MoS_2 sample grown by CVD method. Carrier thermalization occurs within 20 fs and the subsequent cooling of Fermi–Dirac carrier distribution occurs on the ~ 0.6 ps timescale.[85] (d) Pump–probe spectroscopy performed on mechanically exfoliated MoS_2 sample with 452 nm pump and 905 nm probe, showing the dependence of the timescales on the layer number. Different curves are scaled in magnitude for clarity.[86]

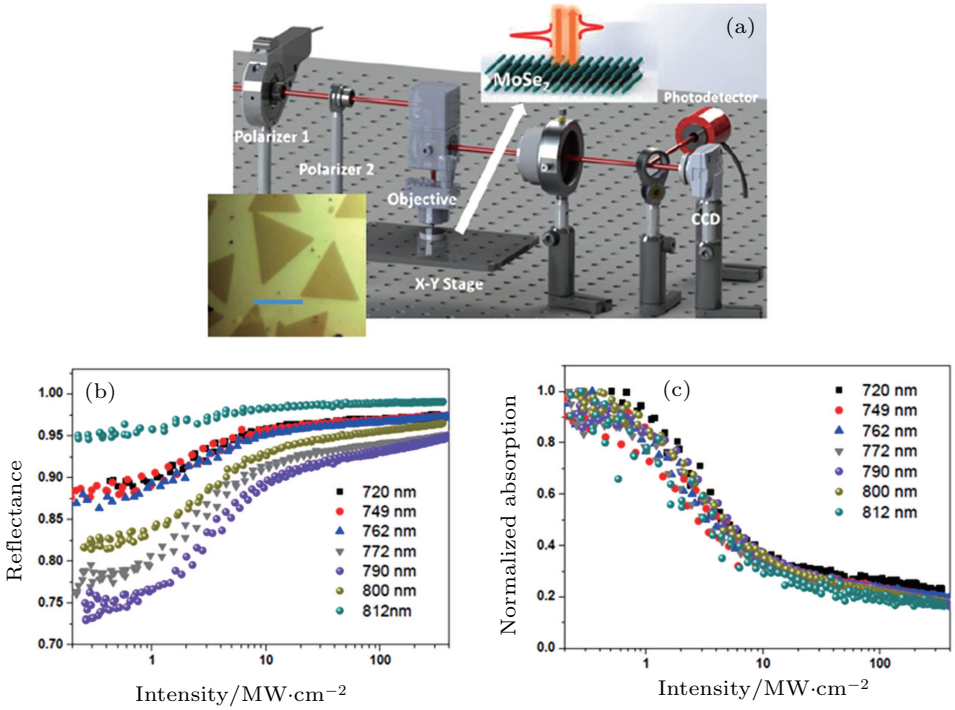

Fig. 7. (color online) (a) Schematic setup of a microscopic nonlinear optical absorption setup. Inset shows optical micrograph of $MoSe_2$ on silver mirror (scale bar, 20 μm). (b) Nonlinear reflectance and (c) normalized absorption of monolayer $MoSe_2$ on silver mirror, showing uniform nonlinear optical characteristics (a modulation depth of ∼ 80% and a saturation intensity ∼ 2.5 MW/cm^2) over the broad spectral range 720–812 nm.[88]

For pulsed laser applications, TMD-enabled pulsed laser was first demonstrated by Zhang and co-workers in early 2014, where few-layer MoS_2 obtained by hydrothermal method was used to mode-lock a Yb-doped fiber laser operating at 1054.3 nm, though a relatively long pulse duration of ∼ 800 ps was obtained.[89] Soon after the first report, Luo and Xu *et al.* demonstrated femtosecond pulse generation (∼ 700 fs) using a MoS_2-PVA composite absorber in an Er-doped ring cavity.[90] A number of reports followed, unambiguously verifying the capability of TMDs as effective saturable absorbers for fiber lasers operating across the visible to the near infrared range ∼ 2 μm.[91–103] In particular, broadband operation is manifested in the demonstration of a wavelength-tunable Q-switched regime,[91] a wavelength-tunable mode-locked regime[92] and a single MoS_2 device-enabled, Q-switched, Yb-, Er-, and Tm-doped fiber laser across 1–2 μm.[93] While the initial studies primarily employed MoS_2 as the SA material, other TMD materials such as WS_2[98–101] and $MoSe_2$[102,103] have also been demonstrated. The earliest study on the ultrafast nonlinear optical properties of TMDs revealed strong nonlinear absorption of MoS_2 in the visible and infrared range (see Fig. 8).[89,104] As with the relaxation dynamics, nonlinear optical characteristics are also dependent on material quality. Combining with various methods available for repairing the defects in TMDs,[105] it opens an exciting route of controlling the nonlinear optical properties. Luo and co-workers demonstrated the first Q-switched operation of visible ZBLAN fiber lasers, employing a range of LPE-processed TMD materials. The red-light passive Q-switching generated stable pulse trains with the pulse width of ∼ 200 ns and a wide range of repetition rates from 232.7 to 512.8 kHz (see Fig. 9).[84] The demonstration of compact and efficient mode-locked visible lasers, especially for visible diode lasers widely found in the UV and visible band, is of potential broad interest and may mitigate the dependence of bulky and expensive harmonic generation setups based on Ti:sapphire lasers. On the other hand, the sub-bandgap optical absorption has attracted attention as a way to scale the operation of TMDs into the long-wavelength range. A theoretical model based on edge-state absorption that may account for the sub-band gap behaviour of TMDs has been recently proposed.[106] Compared with graphene, TMDs are relatively less explored in solid-state lasers, probably due to the high insertion loss. Very recently, a bulk laser operating close to 3 μm has been demonstrated by using MoS_2's long-wave absorption, and more experimental studies, particularly on the direct revealing of optical signatures of edge states, will help provide more physical foundation for the use of TMDs for long-wavelength operations.[107]

Most of the existing TMD-based pulsed lasers employ LPE for obtaining single- or few-layer TMD flakes. Li and co-workers demonstrated the first mode-locked laser based on a CVD-grown multilayer MoS_2 SA. The authors showed robust mode-locking in an erbium-doped fiber laser, illustrating the potential of using large and uniform, polymer-free material for pulsed laser operation, although the multilayer still has to be transferred onto the fiber ferrule end.[108] Following sim-

ilar CVD growth and transfer methods, Khazaeizhad and co-workers demonstrated an evanescent field interaction device, where both anomalous and normal dispersion cavities were successfully mode-locked for 1.55 μm operation.[109] One advantage of TMD compared with graphene is the compatibility of large-area deposition directly on dielectric substrates, such as quartz and silica. Single crystal material with lateral sizes larger than several tens of microns can now be routinely grown. Devices that are free from transfer processes would be highly desirable, i.e., MoS_2 multilayers directly grown on optical substrate or fiber end, and will greatly facilitate highly repeatable device fabrication.

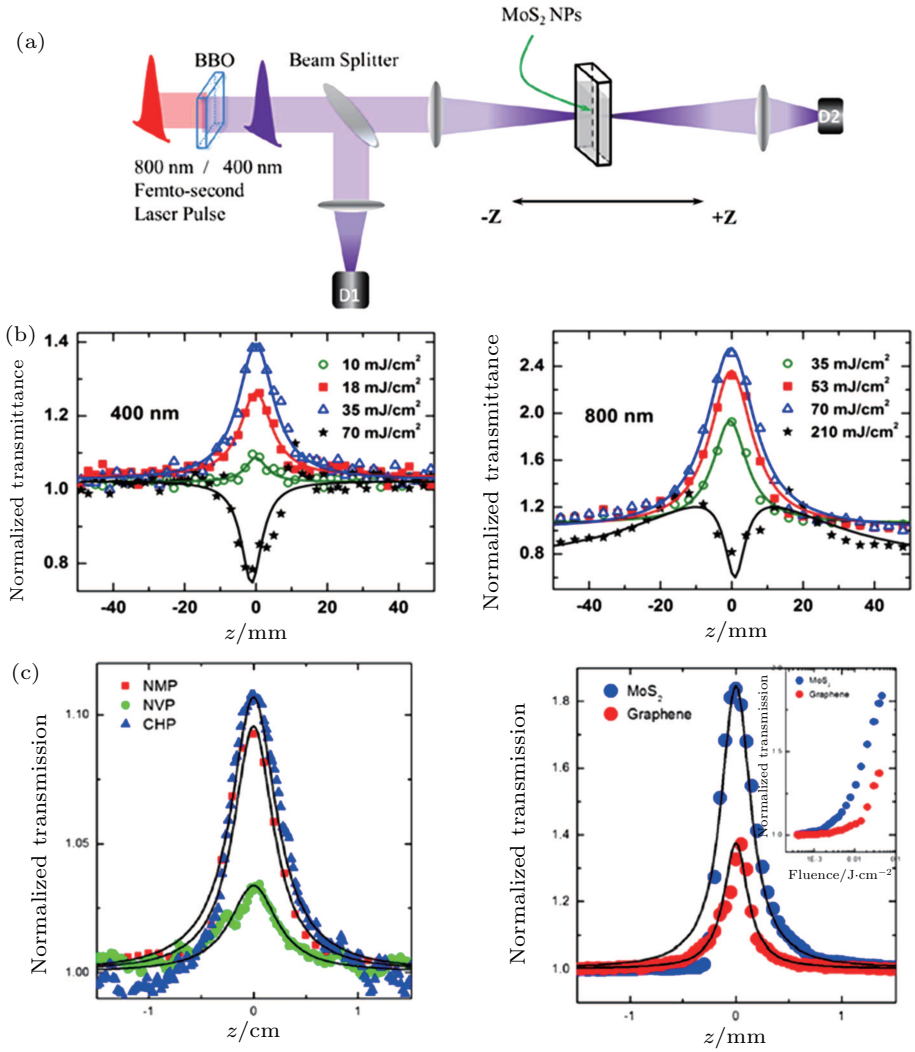

Fig. 8. (color online) (a) Schematic diagram of the Z-scan experimental setup.[89] (b) open-aperture *Z*-scan measurements of MoS_2 dispersions in a 1-mm cuvette at 400 nm (left) and 800 nm (right) with different input fluences.[89] (c) Open-aperture *Z*-scan results of the MoS_2 dispersions under the excitation of 100 fs pulses at 800 nm in different solvents, showing clear influence nonlinear optical characteristics from the environment (left), and comparison of nonlinear performance of MoS_2 ($T = 34.4\%$) and graphene ($T = 16.5\%$) dispersions (right), where MoS_2 shows a stronger modulation depth. Inset: normalized transmission as a function of fluence.[104]

Since graphene was identified as a promising SA material, topological insulators (Tis), another mainstream category of Dirac materials that have drawn broad attention in the field of condensed-matter physics have been identified as potential saturable absorber materials (such as Bi_2Te_3,Bi_2Se_3, Sb_2Te_3, etc.).[110–119] This review however will not summarize those results in detail as similar results were demonstrated following the same vein as with graphene absorbers, though the first report of TI-based SA preceded those of TMDs.[91] In the following we focus on the recently emerging black phosphorus which has become the new focus of the field.

2.3. Black phosphorus (BP)

Black phosphorus (BP), the most thermodynamically stable allotrope of the element phosphorus, was recently rediscovered as an intriguing two-dimensional material as motivated by the demonstration of a BP-based field-effect transistor by Zhang and co-workers.[120] For photonics applications, BP's unique strength lies in its layer-dependent direct bandgap, i.e., from ~ 0.3 eV (bulk form) to ~ 2.0 eV (monolayer), which provides an effective bridge between the energy gap of the semi-metallic graphene and the relatively large band gap TMDs.[121] In addition to its tunable bandgap

and high carrier mobility, the structural anisotropy of BP leads to highly anisotropic mechanical, electrical, and optical properties.[122,123] A number of electronic and optoelectronic applications based on BP and its heterostructures have been developed thus far.[124,125] For example, a BP-based photodetector that can respond to mid-infrared light ~3.39 μm with a high responsivity of ~ 82 A/W was recently demonstrated,[126] showing great potential for chip-scale mid-infrared sensing and imaging applications based on the inherent advantages offered by this emerging 2D material.

Due to its relatively narrow direct bandgap, multilayer BP was considered a promising saturable absorber for the long wavelength range, where light–matter interactions in graphene and TMDs are not as strong. BP nanoplatelets dispersed in different solvents obtained by liquid phase exfoliation method[127] were first investigated by *Z*-scan technique across a broad spectral range, spanning 400–1930 nm.[128] Regardless of the characterization wavelength and pulse duration (femtosecond or picosecond), the BP-based saturable absorbers are found to exhibit quite large modulation depth (> 10%), though the saturation intensity deduced from the femtosecond Z-scan measurement is quite high, about several hundreds of GW/cm^2. On the other hand, a few studies on the photocarrier relaxation dynamics in BP have been reported.[129–131] While angle-sensitive transient effects were identified in all three pump–probe studies, the present results do not converge to a unified physical picture by which photocarriers' dynamics can be well accounted for. Further investigation of BP's photocarrier excitation and relaxation would be important for understanding their detailed nonlinear optical behavior.

For short-pulsed laser applications, mechanically exfoliated BP was first used as a saturable absorber to enable both Q-switched and mode-locked operations for a telecom band Er-doped fiber laser ~ 1.55 μm.[132] Inspiringly, the nonlinear optical characteristics of the exfoliated sample can be effectively tuned through layer thickness control, i.e., the modulation depth in transmittance can be changed from 8% (thin sample) to 18.5% (thick sample). The operation wavelength of BP-enabled pulsed laser was soon extended to the thulium fiber band ~ 1.9–2.0 μm, where a mechanically exfoliated thin film of BP (about 300 nm in thickness) was deposited directly onto the fiber ferrule end.[133] The thulium laser generates 739 fs pulses, with a ~ 36.8 MHz repetition rate and 1.5 mW output power, which corresponds to a pulse energy of 80 pJ. No damage or degradation was observed for the BP saturable absorber at this operation condition. To mitigate the potential damage caused by direct laser irradiation, evanescent field interaction was employed, where the BP is deposited either on micro-fiber or D-shape fibers. A number of Q-switched or mode-locked lasers operating in the 1–1.55 μm range were demonstrated using this scheme.[134–137] By fabricating a BP saturable absorber mirror, Zhang and co-workers demonstrated the first mode-locked bulk laser operating at a wavelength of 1064 nm. The pulse duration is relatively long ~ 6.1 ps, with an average output power of 460 mW.[138] Through intra-cavity dispersion control, the pulse duration and output power were significantly optimized, with 272 fs pulses and a peak power approaching 24 MW achieved.[139] Thus far, the longest wavelength bulk laser enabled by a BP absorber is a passively Q-switched Cr:ZnSe laser operating at a wavelength around 2.4 μm, where pulses as short as 189 ns were achieved, corresponding to a pulse energy of 205 nJ.[140]

Qin and co-workers were the first to achieve 3 μm operation by using LPE processed BP-NMP solution. A reflective device is fabricated by dropping the solution onto a gold-coated mirror and drying it in a cabinet (80% reflectance at 2.9 μm). An Er:ZBLAN fiber laser operating at 2.78 μm was successfully Q-switched with pulse width around 1.2 μs, and the BP SAM device was used as a cavity mirror (free-space coupled).[141] By transferring a mechanically exfoliated BP onto the gold-coated mirror, mode-locked operation at 2.78 μm was subsequently obtained with a pulse duration of 42 ps, a repetition rate of 24 MHz, which are similar to those achieved by graphene-based absorbers.[142] Through thickness characterization, the BP flake was found to be ~143 nm, corresponding to ~238 layers. According to the bandgap equation, a bandgap of 0.33 eV is inferred, which means an operating range up to 3.8 μm is possible.[142] It should be noted that the measured modulation depth and saturation intensity is about 19% and 9 μJ/cm^2, respectively (Fig. 10). More recently, LPE-processed BP was used to enable a 2.97-μm mode-locked ZBLAN fiber laser with 8.6 ps pulses, which represents the longest mode-locking wavelength for BP-based pulsed lasers.[143] The authors studied the long-term stability of the laser and found that due to the degradation of the BP (mainly through interaction with oxygen and water molecules[144]), the laser can operate stably within about three days. This relatively poor environmental stability needs to be dramatically improved to match the level of standard semiconductor-based devices. Among others, the nonlinear optical properties of BP in the mid-infrared, particularly beyond 3 μm, has remained less well characterized and studies of this topic will help provide more solid evidence for its potential use as a mid-infrared saturable absorber material. Due to BP's exciting prospect for novel nanoelectronic and nanophotonic applications, increasing efforts are dedicated to improving the material's environmental stability.[145–147] Large-area growth and advances in passivation and stability enhancement will undoubtedly strengthen the further application of BP in the area of lasers and photonics.

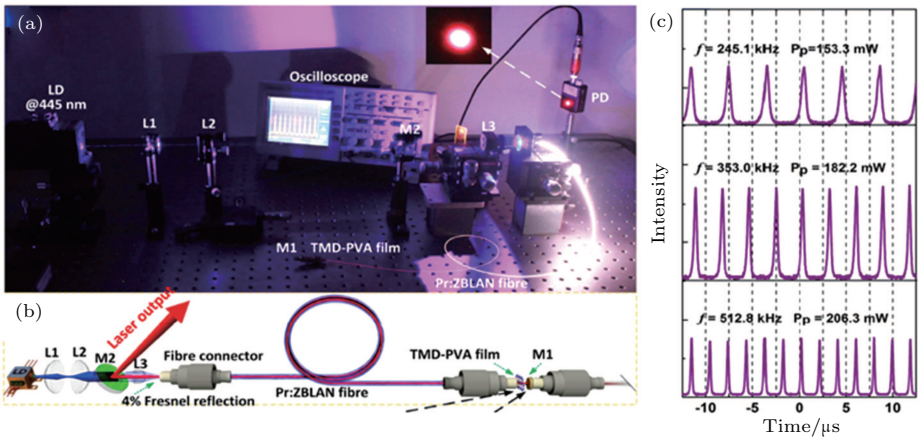

Fig. 9. (color online) (a) Photograph of the passively Q-switched visible fibre laser. Inset: the output beam spot. (b) Schematic of the visible fiber laser. (c) Q-switched pulse trains under different pump powers.[84]

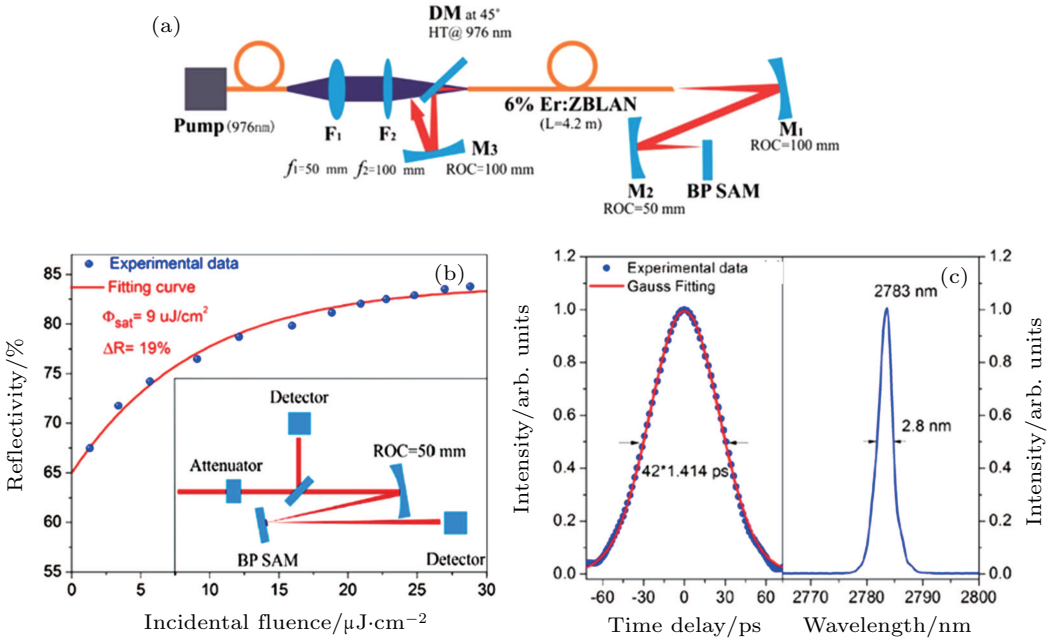

Fig. 10. (color online) (a) Schematic diagram of the BP mode-locked Er:ZBLAN fiber laser. (b) Saturable absorption measurement of BP SAM at 2.8 μm. Inset: experimental setup for the nonlinear absorption measurement. (c) Autocorrelation trace of the mode-locked pulses as well as the corresponding mode-locked optical spectrum.[142]

3. Challenges and outlook

The unique set of optical properties of emerging two-dimensional materials have established them as a technologically important category of materials that hold great potential to be exploited for cost-effective and broadband saturable absorbers. The question of whether one particular material would stand out from the relatively broad range of materials is still open to debate. Nevertheless, to be used as a versatile optical switch that will be amendable for different laser formats, some generic requirements apply. These include the reliability and repeatability of material growth; whether large area and uniform materials can be grown on arbitrary optical substrates (preferably without the need of transfer); whether the nonlinear optical features could be precisely and flexibly controlled; and if the material can tolerate high laser intensities at a variety of laser wavelengths and pulse durations. As it currently stands, while some of the requirements are adequately met by emerging 2D materials, not all criteria have been fulfilled in one specific material yet. For example, graphene possesses advantages in large-area and reliable growth based on CVD method. However, the difficulty with which to precisely control the layer number and the relatively weak light–matter interaction, limit its potential in scenarios where both a large absolute absorption and strong modulation depth are needed. Employing a capacitor-like device or optical resonance designs have shown flexible and precise control of nonlinear optical characteristics of graphene, including both modulation depth and linear absorption, but this is normally at the expense of more complex device geometry and transient characteristics of graphene are hard to customize over a large

temporal range. The inherent excitonic features of TMDs dictate they can act as effective visible or UV saturable absorber with strong light–matter interaction. The fact that TMDs can be directly deposited on common dielectric substrates means they have a great potential for scalable fabrication, which has definitive advantages than devices made with alternative methods, such as mechanical exfoliation. However, the control of the nonlinear optical response of TMDs is not fully understood and requires further investigation. Using them to enable mode-locked visible laser, especially visible diode lasers widely found in the UV and visible band is of potential broad interests. In the case of BP, it should be mentioned that pulsed laser results are fast approaching those obtained by graphene and TMDs, although the first BP-enabled laser demonstrator is reported only in 2015. Enhancement of the stability of BP is still a prerequisite for the material to significantly expand its prospect for technological applications. Long-term stability optimization would remain a key aspect for BP-enabled devices. Compared to graphene and TMDs, one unique opportunity for BP arises from the fact that a relatively large number of layers is usually synergetic with functionality design. The thickness of a few hundred nanometers would comfortably allow chemical composition engineering to play a more active role in BP-based devices, compared with other few-layer 2D materials. Finally, for the emerging 2D materials to be reliably applied in optical or optoelectronic devices, the effects from adjacent layered materials or substrates (including passivation layers) have to be systematically studied.

In summary, ultrafast lasers enabled by emerging 2D materials have become a highly active field of research, where significant efforts have been dedicated to the demonstration of pulsed lasers with improved output characteristics including duration, repetition rates, average power and peak power. Revealing the underlying photo-physics together with the engineering of highly robust and tunable materials will help set the stage for these novel materials to be further exploited in practical applications, including not only ultrafast saturable absorbers, but also photodetectors, modulators and light-emitting devices.

Acknowledgments

The author is grateful for helpful discussion with Chunhui Zhu.

References

[1] Letokhov V S 1985 *Nature* **316** 325
[2] Shah J 1996 *Ultrafast Spectroscopy of Semiconductors and Semiconductor Nanostructures*, vol. 115 (Springer Science & Business Media)
[3] Keller U 2003 *Nature* **424** 831
[4] Jackson S D 2012 *Nat. Photon.* **6** 423
[5] Schliesser A, Picqué N and Hänsch T W 2012 *Nat. Photon.* **6** 440
[6] Zhao K, Zhang Q, Chini M, Wu Y, Wang X and Chang Z 2012 *Opt. Lett.* **37** 3891
[7] Sansone G, Benedetti E, Calegari F, Vozzi C, Avaldi L, Flammini R, Poletto L, Villoresi P, Altucci C, Velotta R, Stagira S, Silvestri S De and Nisoli M 2006 *Science* **314** 443
[8] Man M K l, Margiolakis A, Deckoff-Jones S, Harada T, Wong E L, Krishna M B M, Madó J, Winchester A, Lei S, Vajtai R, Ajayan P M and Dani K M 2017 *Nat. Nanotechnol.* **12** 36
[9] Chini M, Zhao K and Chang Z 2014 *Nat. Photon.* **8** 178
[10] Krausz F and Stockman M I 2014 *Nat. Photon.* **8** 205
[11] Haus H A, Fujimoto J G and Ippen E P 1991 *J. Opt. Soc. Am. B* **8** 2068
[12] Rafailov E U, Cataluna M A and Sibbett W 2007 *Nat. Photon.* **1** 395
[13] Fermann M E and Hartl I 2013 *Nat. Photon.* **7** 868
[14] Tilma B W, Mangold M, Zaugg C A, Link S M, Waldburger D, Klenner A, Mayer A S, Gini E, Golling M and Keller U 2015 *Light: Sci. Appl.* **4** e310
[15] Keller U, Weingarten K J, Kartner F X, Kopf D, Braun B, Jung I D and Der Au J A 1996 *IEEE J. Sel. Top. Quantum Electron* **2** 435
[16] Zitter R N 1969 *Appl. Phys. Lett.* **14** 73
[17] DeMaria A J, Stetser D A and Heynau H 1966 *Appl. Phys. Lett.* **8** 174
[18] Kalisky Y 2004 *Prog. Quantum Electron.* **28** 249
[19] Camargo M B, Kokta M, Stultz R D and Birnbaum M 1995 *Opt. Lett.* **20** 339
[20] Spence D E, Kean P N and Sibbett W 1991 *Opt. Lett.* **16** 42
[21] Keller U, Miller D A B, Boyd G D, Chiu T H, Ferguson J F and Asom M T 1992 *Opt. Lett.* **17** 505
[22] Haiml M, Siegner U, Morier-Genoud F, Keller U, Luysberg M, Lutz R C, Specht P and Weber E R 1999 *Appl. Phys. Lett.* **74** 3134
[23] Delpon E L, Oudar J L, Bouché N, Raj R, Shen A, Stelmakh N and Lourtioz J M 1998 *Appl. Phys. Lett.* **72** 759
[24] Novoselov K S, Geim A K, Morozov S V, Jiang D, Zhang Y, Dubonos S V, Grigorieva I V and Firsov A A 2004 *Science* **306** 666
[25] Geim A K and Novoselov K S 2007 *Nat. Mater.* **6** 183
[26] Avouris P 2010 *Nano Lett.* **10** 4285
[27] Bonaccorso F, Sun Z, Hasan T and Ferrari A C 2010 *Nat. Photon.* **4** 611
[28] Novoselov K S, Fal V I, Colombo L, Gellert P R, Schwab M G and Kim K 2012 *Nature* **490** 192
[29] Bao Q, Zhang H, Wang Y, Ni Z, Yan Y, Shen Z X, Loh P K and Tang D Y 2009 *Adv. Funct. Mater.* **19** 3077
[30] Sun Z, Hasan T, Torrisi F, Popa D, Privitera G, Wang F, Francesco B, Basko D M and Ferrari A C 2010 *ACS Nano* **4** 803
[31] Hasan T, Sun Z, Wang F, Bonaccorso F, Tan P H, Rozhin A G and Ferrari A C 2009 *Adv. Mater.* **21** 3874
[32] Set S Y, Yaguchi H, Tanaka Y and Jablonski M 2004 *IEEE J. Sel. Top. Quant. Electron.* **10** 137
[33] Wang F, Rozhin A G, Scardaci V, Sun Z, Hennrich F, White I H, Milne W I and Ferrari A C 2008 *Nat. Nanotechnol.* **3** 738
[34] D Popa, Sun Z, Hasan T, Torrisi F, Wang F and Ferriari A C 2011 *Appl. Phys. Lett.* **98** 073106
[35] Sun Z, Popa D, Hasan T, Torrisi F, Wang F, Kelleher E J, Travers J C, Nicolosi V and Ferrari A C 2010 *Nano Res.* **3** 653
[36] Fu B, Hua Y, Xiao X, Zhu H, Sun Z and Yang C 2014 *IEEE J. Sel. Top. Quant.* **20** 411
[37] Sotor J, Sobon G, Tarka J, Pasternak I, Krajewska A, Strupinski W and Abramski K M 2014 *Opt. Express* **22** 5536
[38] Martinez A and Yamashita S 2011 *Opt. Express* **19** 6155
[39] Zhang H, Tang D, Knize R J, Zhao L, Bao Q and Loh K P 2010 *Appl. Phys. Lett.* **96** 111112
[40] Tan W D, Su C Y, Knize R J, Xie G Q, Li L J and Tang D Y 2010 *Appl. Phys. Lett.* **96** 031106
[41] Xu J L, Li X L, Wu Y Z, Hao X P, He J L and Yang K J 2011 *Opt. Lett.* **36** 1948
[42] Cho W B, Kim J W, Lee H W, Bae S, Hong B H, Choi S Y, Baek I H, Kim K, Yeom D and Rotermund F 2011 *Opt. Lett.* **36** 4089
[43] Ma J, Xie G Q, Lv P, Gao W L, Yuan P, Qian L J, Yu H H, Zhang H J, Wang J Y and Tang D Y 2012 *Opt. Lett.* **37** 2085
[44] Lagatsky A A, Sun Z, Kulmala T S, Sundaram R S, Milana S, Torrisi F, Antipov O L, Lee Y, Ahn J H, Brown C T A, Sibbett W and Ferrari A C 2013 *Appl. Phys. Lett.* **102** 013113

[45] Mary R, Brown G, Beecher S J, Torrisi F, Milana S, Popa D, Hasan T, Sun Z, Lidorikis E, Ohara Seiki, Ferrari A C and Kar A K 2013 *Opt. Express* **21** 7943

[46] Zaugg C A, Sun Z, Wittwer V J, Popa D, Milana S, Kulmala T S, Sundaram R S, Mangold M, Sieber O D, Golling M, Lee Y, Ahn J H, Ferrari A C and Keller U 2013 *Opt. Express* **21** 31548

[47] Husaini S and Bedford R G 2014 *Appl. Phys. Lett.* **104** 161107

[48] Martinez A and Sun Z 2013 *Nat. Photon.* **7** 842

[49] Sun Z, Hasan T and Ferrari A C 2012 *Physica E* **44** 1082.

[50] Cheng Z, Qin C, Wang F, He H and Goda K 2016 *Front. Optoelectron.* **9** 259

[51] Mattevi C, Eda G, Agnoli S, Miller S, Mkhoyan K A, Celik O, Mastrogiovanni D, Granozzi G, Garfunkel E and Chhowalla M 2009 *Adv. Funct. Mater.* **19** 2577

[52] Hasan T, Sun Z, Tan P, Popa D, Flahaut E, Kelleher E J, Bonaccorso F, Wang F Q, Jiang Z, Torrisi F and Privitera G 2014 *ACS Nano* **8** 4836

[53] Kivistö S, Hakulinen T, Kaskela A, Aitchison B, Brown D P, Nasibulin A G, Kauppinen E I, Härkönen A and Okhotnikov O G 2009 *Opt. Express* **17** 2358

[54] Zhang M, Kelleher E J R, Pozharov A S, Obraztsova E D, Popov S V and Taylor J R 2011 *Opt. Lett.* **36** 3984

[55] Wang F Q, Torrisi F, Jiang Z, Popa D, Hasan T, Sun Z and Ferrari A C 2012 *Proceedings of Conference on Lasers and Electro-Optics*, May 6–11, 2012, Baltimore, USA, p. JW2A.72

[56] Zhang M, Kelleher E J R, Torrisi F, Sun Z, Hasan T, Popa D, Wang F Q, Ferrari A C, Popov S V and Taylor J R 2012 *Opt. Express* **20** 25077

[57] Wei C, Zhu X S, Wang F Q, Xu Y, Balakrishnan K, Song F, Norwood R A and Peyghambarian N 2013 *Opt. Lett.* **38** 3233

[58] Zhu G W, Zhu X S, Wang F Q, Xu S, Li Y, Guo X L, Balakrishnan K, Norwood R A and Peyghambarian N 2016 *IEEE Photon. Technol. Lett.* **28** 7

[59] Cizmeciyan M N, Kim J W, Bae S, Hong B H, Rotermund F and Sennaroglu A 2013 *Opt. Lett.* **38** 341

[60] Tolstik N, Sorokin E and Sorokina I T 2014 *Opt. Express* **22** 5564

[61] Tolstik N, Pospischil A, Sorokin E and Sorokina I T 2014 *Opt. Express* **22** 7284

[62] Cho W B, Choi S Y, Zhu C H, Kim M H, Kim J W, Kim J S, Park H J, Shin D H, Jung M Y, Wang F Q and Rotermund F 2016 *Opt. Express* **18** 20774

[63] Wang Q, Teng H, Zou Y, Zhang Z, Li D, Wang R, Gao C Q, Lin J J, Guo L W and Wei Z 2012 *Opt. Lett.* **37** 395

[64] Crombie C, Walsh D A, Lu W, Zhang S, Zhang Z, Kennedy K, Calvez S, Sibbett W and Brown C T A 2012 *Opt. Express* **20** 18138

[65] Lee E J, Choi S Y, Jeong H, Park N H, Yim W, Kim M H, Park J K, Son S, Bae S, Kim S J and Lee K 2015 *Nat. Commun.* **6** 6851

[66] Baylam I, Cizmeciyan M N, Ozharar S, Polat E O, Kocabas C and Sennaroglu A 2014 *Opt. Lett.* **39** 5180

[67] Leitner M, Glas P, Sandrock T, Wrage M, Apostolopoulos G, Riedel, Kostial A H, Herfort J, Friedland K J and Däweritz L 1999 *Opt. Lett.* **24** 1567

[68] Lederer M J, Kolev V, Luther-Davies B, Tan H H and Jagadish C 2001 *J. Phys. D: Appl. Phys.* **34** 2455

[69] Wang Q H, Kalantar-Zadeh K, Kis A, Coleman J N and Strano M S 2012 *Nat. Nanotechnol.* **7** 699

[70] Mak K F and Shan J 2016 *Nat. Photon.* **10** 216

[71] Duan X, Wang C, Pan A, Yu R and Duan X 2015 *Chem. Soc. Rev.* **44** 8859

[72] Radisavljevic B, Radenovic A, Brivio J, Giacometti I V and Kis A 2011 *Nat. Nanotechnol.* **6** 147

[73] Mak K F, Lee C, Hone J, Shan J and Heinz T F 2010 *Phys. Rev. Lett.* **105** 136805

[74] Ramasubramaniam A 2012 *Phys. Rev. B* **86** 115409

[75] Mak K F, He K, Lee C, Lee G H, Hone J, Heinz T F and Shan J 2013 *Nat. Mater.* **12** 207

[76] Qiu D Y, Felipe H and Louie S G 2013 *Phys. Rev. Lett.* **111** 216805

[77] Ugeda M M, Bradley A J, Shi S F, Felipe H, Zhang Y, Qiu D Y, Ruan W, Mo S K, Hussain Z, Shen Z X, Wang F, Louie A G and Crommie M F 2014 *Nat. Mater.* **13** 1091

[78] Chernikov A, Ruppert C, Hill H M, Rigosi A F and Heinz T F 2015 *Nat. Photon.* **9** 466

[79] Pogna E A A, Marsili M, Fazio D D, Conte S D, Manzoni C, Sangalli D Yoon D, Lombardo A, Ferrari A C, Marini A, Cerullo G and Prezzi D 2016 *ACS Nano* **10** 1182

[80] Kumar N, Cui Q, Ceballos F, He D, Wang Y and Zhao H 2014 *Phys. Rev. B* **89** 125427

[81] Sun D, Rao Y, Reider G A, Chen G, You Y, Brézin L and Heinz T F 2014 *Nano Lett.* **14** 5625

[82] Wang R, Ruzicka B A, Kumar N, Bellus M Z, Chiu H Y and Zhao H 2012 *Phys. Rev. B* **86** 045406

[83] Shi H, Yan R, Bertolazzi S, Brivio J, Gao B, Kis A, Jena D, Xing H and Huang L 2013 *ACS Nano* **7** 1072

[84] Luo Z Q, Wu D D, Xu B, Xu H Y, Cai Z P, Peng J, Weng J, Xu S, Zhu C H, Wang F Q, Sun Z P, Zhang H and Sun Z 2016 *Nanoscale* **8** 1066

[85] Nie Z G, Long R, Sun L F, Huang C C, Zhang J, Xiong Q H, Hewak D W, Shen Z X, Prezhdo O V and Loh Z H 2014 *ACS Nano* **8** 10931

[86] Wang H, Zhang C and Rana F 2015 *Nano Lett.* **15** 8204

[87] Xu S, Wang F Q, Zhu C H, Meng Y F, Liu Y J, Liu W Q, Tang J Y, Liu K H, Hu G H, Howe R C T H and Hasan T 2016 *Nanoscale* **8** 9304

[88] Nie Z, Kelleher E, Liu K, Xu Y and Wang F 2016 *Proceedings of Conference on Lasers and Electro-Optics (CLEO)*, June 5–10, 2016, San Jose, USA, p. FTu1A.1

[89] Zhang H, Lu S B, Zheng J, Du J, Wen S C, Tang D Y and Loh K P 2014 *Opt. Express* **22** 7249

[90] Liu H, Luo A P, Wang F Z, Tang R, Liu M, Luo Z C, Xu W C, Zhao C J and Zhang H 2014 *Opt. Lett.* **39** 4591

[91] Woodward R I, Kelleher E J R, Howe R C T, Hu G, Torrisi F, Hasan T, Popov S V and Taylor J R 2014 *Opt. Express* **22** 31113

[92] Zhang M, Howe R C, Woodward R I, Kelleher E J, Torrisi F, Hu G H, Popov S V, Taylor J R and Hasan T 2015 *Nano Res.* **8** 1522

[93] Luo Z, Huang Y, Zhong M, Li Y, Wu J, Xu B, Xu H Y, Cai Z P, Peng J and Weng J 2014 *J. Lightwave Technol.* **32** 4077

[94] Liu M, Zheng X W, Qi Y L, Liu H, Luo A P, Luo Z C, Xu W C, Zhao C J and Zhang H 2014 *Opt. Express* **22** 22841

[95] Wang Y, Mao D, Gan X, Han L, Ma C, Xi T, Zhang Y, Shang W Y, Hua S J and Zhao J 2015 *Opt. Express* **23** 205

[96] Tian Z, Wu K, Kong L, Yang N, Wang Y, Chen R, Hu W S, Xu J Q and Tang Y 2015 *Laser Phys. Lett.* **12** 065104

[97] Li H, Xia H, Lan C, Li C, Zhang X, Li J and Liu Y 2015 *IEEE Photon. Technol. Lett.* **27** 69

[98] Mao D, Wang Y, Ma C, Han L, Jiang B, Gan X T, Hua S J, Zhang W D, Mei T and Zhao J 2015 *Sci. Rep.* **5** 7965

[99] Yan P, Liu A, Chen Y, Chen H, Ruan S, Guo C, Chen S, Li L, Yang H P, Hu J G and Cao G 2015 *Opt. Mater. Express* **5** 479

[100] Wu K, Zhang X, Wang J, Li X and Chen J 2015 *Opt. Express* **23** 11453

[101] Zhang M, Hu G, Howe R C T, Chen L, Zheng Z and Hasan T 2015 *Sci. Rep.* **5** 17482

[102] Luo Z, Li Y, Zhong M, Huang Y, Wan X, Peng J and Weng J 2015 *Photon. Res.* **3** A79

[103] Woodward R I, Howe R C T, Runcorn T H, Hu G, Torrisi F, Kelleher E J R and Hasan T 2015 *Opt. Express* **23** 20051

[104] Wang K, Wang J, Fan J, Lotya M, O'Neill A, Fox D and Zhang H 2013 *ACS Nano* **7** 9260

[105] Yu Z, Pan Y, Shen Y, Wang Z, Ong Z Y, Xu T, Xin R, Pan L J, Wang B G, Sun L T and Wang J 2014 *Nat. Commun.* **5** 5290

[106] Trushin M, Kelleher E J and Hasan T 2016 *Phys. Rev. B* **94** 155301

[107] Fan M, Li T, Zhao S, Li G, Ma H, Gao X, Kränkel C and Huber G 2016 *Opt. Lett.* **41** 540

[108] Xia H, Li H, Lan C, Li C, Zhang X, Zhang S and Liu Y 2014 *Opt. Express* **22** 17341

[109] Khazaeizhad R, Kassani S H, Jeong H, Yeom D I and Oh K 2014 *Opt. Express* **22** 23732

[110] Zhao C, Zhang H, Qi X, Chen Y, Wang Z, Wen S and Tang D 2012 *Appl. Phys. Lett.* **101** 211106

[111] Zhao C, Zou Y, Chen Y, Wang Z, Lu S, Zhang H, Wen S and Tang D 2012 *Opt. Express* **20** 27888

[112] Luo Z C, Liu M, Liu H, Zheng X W, Luo A P, Zhao C J, Zhang H, Wen S C and Xu W C 2013 *Opt. Lett.* **38** 5212

[113] Luo Z, Huang Y, Weng J, Cheng H, Lin Z, Xu B, Cai Z P and Xu H 2013 *Opt. Express* **21** 29516

[114] Lin Y H, Yang C Y, Lin S F, Tseng W H, Bao Q, Wu C I and Lin G R 2014 *Laser Phys. Lett.* **11** 055107

[115] Liu M, Zhao N, Liu H, Zheng X W, Luo A P, Luo Z C, Xu W C, Zhao C J, Zhang H and Wen S C 2014 *IEEE Photon. Technol. Lett.* **26** 983

[116] Luo Z, Liu C, Huang Y, Wu D, Wu J, Xu H, Cai Z P, Lin Z Q, Sun L P and Weng J 2014 *IEEE J. Sel. Top. Quant.* **20** 1

[117] Sotor J, Sobon G and Abramski K M 2014 *Opt. Express* **22** 13244
[118] Jung M, Lee J, Koo J, Park J, Song Y W, Lee K, Lee S B and Lee J H 2014 *Opt. Express* **22** 7865
[119] Lee J, Koo J, Jhon Y M and Lee J H 2014 *Opt. Express* **22** 6165
[120] Li L, Yu Y, Ye G J, Ge Q, Ou X, Wu H, Feng D, Chen X and Zhang Y 2014 *Nat. Nanotechnol.* **9** 372
[121] Xia F, Wang H, Xiao D, Dubey M and Ramasubramaniam A 2014 *Nat. Photon.* **8** 899
[122] Wei Q and Peng X 2014 *Appl. Phys. Lett.* **104** 251915
[123] Wang X, Jones A M, Seyler K L, Tran V, Jia Y, Zhao H, Wang H, Yang L, Xu X and Xia F 2015 *Nat. Nanotechnol.* **10** 517
[124] Castellanos-Gomez A 2015 *J. Phys. Chem. Lett.* **6** 4280
[125] Ling X, Wang H, Huang S, Xia F and Dresselhaus M S 2015 *PNAS* **112** 4523
[126] Guo Q, Pospischil A, Bhuiyan M, Jiang H, Tian H, Farmer D, Deng B, Li C, Han S, Wang H and Xia Q 2016 *Nano Lett.* **16** 4648
[127] Hanlon D, Backes C, Doherty E, Cucinotta C S, Berner N C, Boland C, Lee K, Harvey A, Lynch P, Gholamvand Z and Zhang S 2015 *Nat. Commun.* **6** 8563
[128] Lu S B, Miao L L, Guo Z N, Qi X, Zhao C J, Zhang H, Wen S C, Tang D Y and Fan D Y 2015 *Opt. Express* **23** 11183
[129] He J, He D, Wang Y, Cui Q, Bellus M Z, Chiu H Y and Zhao H 2015 *ACS Nano* **9** 6436
[130] Ge S, Li, C Zhang Z, Zhang C, Zhang Y, Qiu J and Sun D 2015 *Nano Lett.* **15** 4650
[131] Suess R J, Jadidi M M, Murphy T E and Mittendorff M 2015 *Appl. Phys. Lett.* **107** 081103
[132] Chen Y, Jiang G, Chen S, Guo Z, Yu X, Zhao C, Zhang H, Bao Q, Wen S, Tang D and Fan D 2015 *Opt. Express* **23** 12823
[133] Sotor J, Sobon G, Kowalczyk M, Macherzynski W, Paletko P and Abramski K M 2015 *Opt. Lett.* **40** 3885
[134] Luo Z C, Liu M, Guo Z N, Jiang X F, Luo A P, Zhao C J, Yu X F, Xu W C and Zhang H 2015 *Opt. Express* **23** 20030
[135] Park K, Lee J, Lee Y T, Choi W K, Lee J H and Song Y W 2015 *Ann. Phys.* **527** 770
[136] Yu H, Zheng X, Yin K and Jiang T 2015 *Appl. Opt.* **54** 10290
[137] Wang Y, Li J, Han L, Lu R, Hu Y, Li Z and Liu Y 2016 *Laser Phys.* **26** 065104
[138] Zhang B, Lou F, Zhao R, He J, Li J, Su X, Ning J and Yang K 2015 *Opt. Lett.* **40** 3691
[139] Su X, Wang Y, Zhang B, Zhao R, Yang K, He J, Hu Q, Jia Z and Tao X 2016 *Opt. Lett.* **41** 1945
[140] Wang Z, Zhao R, He J, Zhang B, Ning J, Wang Y, Su X, Hou J, Lou F, Yang K and Fan Y 2016 *Opt. Express* **24** 1598
[141] Qin Z P, Xie G Q, Zhang H, Zhao C J, Yuan P, Wen S C and Qian L J 2015 *Opt. Express* **23** 24713
[142] Qin Z P, Xie G Q, Zhao C J, Wen S C, Yuan P and Qian L J 2016 *Opt. Lett.* **41** 56
[143] Li J F, Luo H Y, Zhai B, Lu R G, Zhang H and Liu Y 2016 *Sci. Rep.* **6** 30361
[144] Favron A, Gaufrès E, Fossard F, Phaneuf-L'Heureux A L, Tang N Y W, Lévesque P L, Loiseau A, Leonelli R, Francoeur S and Martel R 2015 *Nat. Mater.* **14** 826
[145] Wood J D, Wells S A, Jariwala D, Chen K S, Cho E, Sangwan V K, Liu X L, Lauhon L J, Marks T J and Hersam M C 2014 *Nano Lett.* **14** 6964
[146] Zhou Q H, Chen Q, Tong Y L and Wang J L 2016 *Angew. Chem.* **128** 11609
[147] Yang B C, Wan B S, Zhou Q H, Wang Y, Hu W T, Lv W M, Chen Q, Zeng Z M, Wen F S, Xiang J Y, Yuan S J, Wang J L, Zhang B S, Wang W H, Zhang J Y, Xu B, Zhao Z S, Tian Y J and Liu Z Y 2016 *Adv. Mater.* **28** 9408